# Cross-subject EEG Linear Domain Adaption Based on Batch Normalization and Depthwise Convolutional Neural Network

Guofa Li[a,*], Delin Ouyang[b], Liu Yang[c], Qingkun Li[d], Kai Tian[e], Baiheng Wu[f], Gang Guo[a]

[a] *College of Mechanical and Vehicle Engineering, Chongqing University, 400044, Chongqing, China*
[b] *Institute of Human Factors and Ergonomics, College of Mechatronics and Control Engineering, Shenzhen University, Shenzhen, 518060, China*
[c] *School of Transportation and Logistics Engineering, Wuhan University of Technology, Wuhan, 430063, China*
[d] *State Key Laboratory of Automotive Safety and Energy, School of Vehicle and Mobility, Tsinghua University, Beijing, 100084, China*
[e] *Institute for Transport Studies, University of Leeds, Leeds, LS1 9JT, UK*
[f] *Department of ICT and Natural Science, Norwegian University of Science and Technology, Ålesund, 6009, Norway*

**Abstract**

Electroencephalogram (EEG)-based emotion recognition has been widely used in affective computing. However, the study on improving recognition accuracy across individuals is insufficient. In this study, a new linear domain adaption approach with experiment-level batch normalization and a single-layer depthwise convolutional neural network is proposed. In particular, the experiment-level batch normalization and depthwise convolutional neural network can be integrated as a linear mapping with a scaling parameter and a translation parameter. By linear mapping, difference between subjects in different domain can be effectively diminished, and the mapping parameters can be used to further investigate EEG emotion mechanism. The domain adaption experiments are conducted with SJTU emotion EEG dataset and SJTU emotion EEG dataset-IV, which are divided into source domain and target domain to validate the recognition effect across individuals. Multiple traditional machine learning and deep learning classifiers are used to examine the effectiveness of the proposed approach. By mapping the EEG data from source domain to target domain, the increment of recognition accuracy is up to 61.11% when using the support vector machine classifier. The highest recognition accuracy 97.22% is achieved when using the logistic regression classifier. The scaling and translation parameters in the mapping procedure are then analyzed with statistical methods. It is found that EEG signal waves in the same emotion category are highly similar and EEG data have characteristics including integration of channels and hierarchy of frequency bands. In addition, the experimental results indicate that emotion complexity and emotion sensitiveness of brain cortex regions can affect the correlations between channels.

*Keywords:* Emotion recognition, brain-computer control, domain adaption, electroencephalogram (EEG), machine learning

## 1. Introduction

### *1.1. Background*

Emotion recognition plays a vital role in affective computing. It is believed that the physiological signal to recognize human emotions is a useful way for affective computing. In current studies, electroencephalogram (EEG) signal measurement has been recognized as one of the effective ways to reflect the human emotion state [1],[2],[3], which benefits from its avoidance of human unconscious or conscious interference in emotion expression. To identify EEG emotion signals with higher recognition accuracy and understand the working mechanism of EEG signals is important for EEG-based emotion recognition.

The methods for EEG-based emotion recognition can be concluded as traditional machine learning methods and deep learning methods [4],[5]. In the early stage, EEG-based emotion recognition models are mainly based on traditional machine learning because of its good stability and interpretability. However, with rapid development of deep learning, it's found that deep learning models can achieve better recognition accuracy than traditional machine learning with more complicated model structures. Literature has also proven that deep learning models are beneficial to improve the recognition accuracies of EEG-based emotion recognition methods, compared with shallow machine learning models [6].

Deep learning method are also extensive used for improving recognition accuracy across subjects, which is an important target for EEG-based emotion recognition [7]. The factors that impact cross-subject EEG emotion recognition include EEG individual differences, temporal instability and experimental error [8],[9]. Many previous studies deal with this problem by deep neural network (e.g., domain adaption and transfer learning), which is expected to narrow the gap between individual EEG emotion signals. However, though deep neural network performs well on EEG-based emotion recognition, the poor in-

*This work was supported by the National Natural Science Foundation of China under grant number 52272421.

*Corresponding author
*Email addresses:* liguofa@cqu.edu.cn (Guofa Li), ouyangdelin2021@email.szu.edu.cn (Delin Ouyang), yang.liu@whut.edu.cn (Liu Yang), lqk18@mails.tsinghua.edu.cn (Qingkun Li), tskt@leeds.ac.uk (Kai Tian), baiheng.wu@ntnu.no (Baiheng Wu), guogang@cqu.edu.cn (Gang Guo)

terpretability resulted from its deep layers becomes a difficult issue that hinders the development of deep learning.

### *1.2. Related work*

Given that deep learning methods can achieve high EEG-based emotion recognition accuracy, many previous researchers perform high-accuracy EEG-based emotion recognition by constructing deep neural networks. Maheshwari et al. [10] proposed a rhythm-specific multi-channel deep convolutional neural network (CNN) to recognize EEG emotions in valance-arousal-dominance model. Song et al. [11] proposed a dynamical graph convolutional neural network that facilitated discriminative EEG feature extraction to improve EEG emotion recognition. Yin et al. [12] constructed a fusion model of graph convolutional neural network and long-short term memories neural networks, where graph convolutional neural network was used to extract graph domain features and long-short term memories neural networks were used to memorize the changes of EEG channels relationship. Cui et al. [13] proposed an end-to-end regional-asymmetric convolutional neural network that consists of temporal, regional and asymmetric feature extractors for emotion recognition with an asymmetric differential layer to capture the discriminative information of brain.

Furthermore, deep neural networks are also specifically designed to address the problem about cross-subject EEG emotion recognition. Some researchers utilize the classical network structure and optimized them to suit the cross-subject tasks. For example, Yao et al. [14] proposed a cross-subject emotion training method based on complex networks with visibility graphs, in which spatial and temporal information of EEG data could be characterized to overcome individual differences. Tan et al. [15] proposed a short-term emotion recognition framework based on a spiking neural network model, which could utilize spatio-temporal EEG patterns for subject-independent emotion recognition. Although the above literature has demonstrated the decent performance of deep learning models, e.g., CNN, on EEG emotion recognition, it is difficult to explain how deep learning models work and how EEG signals respond to different emotions, due to the complex computational procedure of deep learning models, e.g., multiple layers.

Apart from classical network models, transfer learning has also been proven to be useful for EEG signals processing. For example, Yang et al. [16] proposed a methodology to develop a Takagi-Sugeno-Kang (TSK) Fuzzy Logic System (FLS), using transductive transfer learning to detect epileptic EEG signals with different distributions. Deng et al. [17] proposed an advanced method for constructing a TSK fuzzy system with enhanced transductive transfer learning to address the distribution problem in EEG datasets. Subsequently, a technique for transfer learning is devised to tackle cross-subject EEG emotion recognition by mitigating individual difference. For instance, Li et al. [18] introduced an EEG-based emotion recognition method that combines a multi-scale residual network (MSRN) with a meta-transfer learning (MTL) strategy. The MTL approach effectively leverages the benefits of meta-learning and transfer learning to narrow the gap in individual differences among subjects. Zhou et al. [19] presented a novel transfer learning framework called prototypical representation based pairwise learning (PR-PL) that aimed to learn discriminative and generalized prototypical representations for emotion recognition across individuals. By formulating emotion recognition as pairwise learning, it reduced the dependence on precise label information. Particularly, domain adaptation methods in transfer learning appear to be highly suitable for cross-subject EEG-based emotion recognition. For example, Quan et al. [20] introduced a cross-subject emotional EEG classification algorithm that utilizes multi-source domain selection and sub-domain adaptation. The proposed multi-source domain selection algorithm aims to identify EEG data from existing subjects that closely align with the target data distribution in both global and sub-domain contexts, which enhances the performance of the transfer learning model on the target subject. Ning et al. [21] proposed a single-source domain adaptive few-shot learning network for EEG emotion recognition across subjects, in which a domain adaptation method was applied to align the data distribution of different subjects. Similarly, Li et al. [9] proposed a domain adaptation method that integrated task-invariant features and task-specific features in a unified framework model to perform subjects' association reinforcement to eliminate individual differences.

However, most of the previous studies focus on high recognition accuracy while ignoring investigation regarding individual EEG emotion response mechanisms. Additionally, as the models used in previous studies are always designed complicatedly, it is difficult to precisely interpret the working procedure and mechanism of models on EEG data. It is also hard to utilize these models to figure out EEG emotion mechanism. These issues lead to the fact that existing studies on high-performance classifiers and brain emotion mechanism have not directly linked up in a unified methodology, even though the motivations of most EEG classifier studies come from the EEG characteristics and response mechanisms [9],[21]. Therefore, utilizing the developed models to further investigate the mechanism is an important topic in the following EEG studies.

### *1.3. Contributions*

In this paper, a new linear domain adaption method based on experiment-level batch normalization (ELBN) and depthwise convolutional neural network (DCNN) is developed. The proposed method is different from existing EEG emotion recognition models. Specifically, it can realize high cross-subject EEG emotion recognition accuracy by linear domain adaption, which simply concludes scaling and translation operations. Therefore, the parameters of scaling and translation can be used not only for linear mapping for domain adaption, but also to investigate the EEG emotion mechanism. The main contributions of this study include:

1) A simplified domain adaption architecture based on ELBN and DCNN was proposed. The linear mapping process, including scaling and translation operations, can effectively narrow the gap between domains and contribute to achieving high cross-subject EEG emotion recognition accuracy. In addition,

the scaling and translation parameters were adopted to investigate EEG emotion mechanism. This attempt links up the emotion recognition and emotion mechanism and extends the applications of machine learning approaches in EEG studies.

2) The waveforms of EEG data were proved to be highly similar as the similarity between EEG data of different subjects could be reinforced by linear mapping process. It reveals that the influence of EEG cross-subject difference could lead to changes on global values of EEG data without intervening wave motion (except amplitude) within a limited temporal range. This finding provides another improvement direction for cross-subject EEG emotion recognition that aligns the amplitude of EEG data or extracts patterns of EEG waveforms to diminish EEG difference.

3) The characteristics of EEG emotion response were investigated in this study. Using parameters in domain adaption, it was found that EEG data have integration of channels and hierarchy characteristic of frequency bands. The influencing factors of channels correlation, including emotion complexity and emotion sensitiveness of brain cortex regions were also found in linear mapping parameters analysis. In particular, these findings are achieved with a novel analysis method that integrates deep learning and statistical analysis.

The remainder of this paper is organized as follows. The next section introduces the datasets and preprocessing procedure of EEG features. Section 3 describes the proposed method in detail. The obtained results are presented and discussed in Section 4 and Section 5, respectively. Finally, the conclusions are presented in Section 6.

## 2. Datasets and features preprocessing

### *2.1. SEED series datasets*

**a) SEED dataset.** SJTU emotion EEG dataset (SEED) was acquired by using the ESI NeuroScan System according to the international 10-20 system [22]. During the experiment procedure, movie clips were presented to each subject in fifteen separate emotion elicitation trials (see Fig. 1). The elicited EEG emotion data were collected from 62 channels at a sampling rate of 1000 Hz.

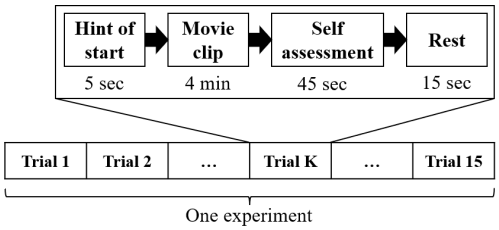


**Fig. 1.** The protocol of experiments in the SEED dataset.

In each trial, a starting hint was given five seconds before the start of each clip. Each movie clip was approximately four minutes. After each clip, subjects had 45 seconds to complete a questionnaire [23] reporting their immediate emotional reactions to the film clips. Subsequently, another fifteen seconds were provided for rest before the start of the next trial. The order of emotions presented in the selected clips was [1, 0, -1, -1, 0, 1, -1, 0, 1, 1, 0, -1, 0, 1, -1], where 1 stood for positive emotion, 0 for neutral, and -1 for negative.

The collected raw EEG data were downsampled to 200 Hz and filtered with a 0-75 Hz frequency band to remove noise and artifacts. Fifteen young subjects (7 males and 8 females; age: 23.27±2.37 years) participated in data collection in the SEED. Each subject repeated the abovementioned data collection procedure three times with an interval of one week or longer. Thus, the collected data in the SEED includes a total of 45 experimental sessions and 675 trials (225 trials for each emotion category). These source data is available for download at: https://bcmi.sjtu.edu.cn/~seed/seed.html.

**b) SEED-IV dataset.** SEED-IV dataset was created with the same devices as the SEED dataset by following a similar experiment workflow [24]. There were totally 24 trials with emotional film clips presented to each subject in one experiment (see Fig. 2). Each film clip had a five seconds hint for starting and a 45 s self-assessment with the positive and negative affect schedule scales [25]. Every subject participated in experiments three times in different periods, and the order of emotions in these three experimental sessions were set as [1, 2, 3, 0, 2, 0, 0, 1, 0, 1, 2, 1, 1, 1, 2, 3, 2, 2, 3, 3, 0, 3, 0, 3], [2, 1, 3, 0, 0, 2, 0, 2, 3, 3, 2, 3, 2, 0, 1, 1, 2, 1, 0, 3, 0, 1, 3, 1], and [1, 2, 2, 1, 3, 3, 3, 1, 1, 2, 1, 0, 2, 3, 3, 0, 2, 3, 0, 0, 2, 0, 1, 0] respectively with 0, 1, 2, and 3 denoted the ground truth, neutral, sad, fear, and happy emotions.

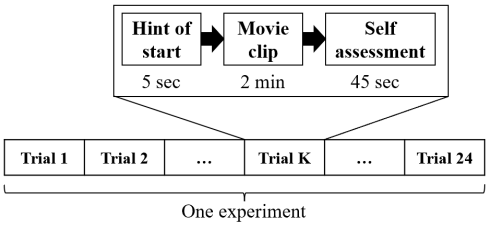


**Fig. 2.** The protocol of experiments in the SEED-IV dataset.

The raw EEG data were recorded at a 1000 Hz sampling rate and a band-pass filter between 1 and 75 Hz was applied to filter the unrelated artifacts. Fifteen subjects (seven males and eight females, aged between 20 and 24 years) participated in data collection in the SEED-IV. As each subject had three experimental sessions, the collected data in the SEED-IV includes a total of 45 experimental sessions and 1080 trials (270 trials for each emotion category). These source data is available for download at: https://bcmi.sjtu.edu.cn/~seed/seed-iv.html.

### *2.2. ELBN for EEG features processing*

To unify the format of EEG inputs of DCNN, PSD features that can show the distribution of signal power [8] were extracted in different frequency bands (i.e., delta: 1-4 Hz, theta: 4-8 Hz, alpha: 8-14 Hz, beta: 14-30 Hz, and gamma: 30-50 Hz) per channel in SEED and SEED-IV and then cut to same-length epochs. In practical operation, PSD features that had been extracted and processed with linear dynamic system in SEED and

SEED-IV were directly applied. According to [22] and [24], PSD features in SEED were extracted with a 1-second time window without overlapping, while PSD features in SEED-IV were extracted with a 4-second time window without overlapping. However, the number of epochs in different trials as well as different datasets are different. Considering to make full use of epochs and unify the inputs format, the extracted PSD features in the front 180 epochs in each trial were selected as an independent sample. Those trials less than 180 epochs were filled with zeros.

Given that ELBN can regulate the baseline of EEG data and diminish EEG individual difference [8],[26], the processed PSD features in one experimental session were then processed with ELBN. Specifically, the PSD features in each frequency band of each channel were normalized within the experimental session by using the following equation,

$$X_{BN_k} = \frac{X_k - X_{min}}{X_{max} - X_{min}} \tag{1}$$

where $X_k$ and $X_{BN_k}$ were the PSD value in an epoch and the corresponding value after applying this ELBN method, respectively. $X_{min}$ and $X_{max}$ were the minimum and maximum values of the PSD feature in each experimental session, respectively.

ELBN approach could be regarded as a linear mapping process by transforming Eq. (1) as:

$$X_{BN_k} = w_{BN} X_k + b_{BN} \tag{2}$$

where $w_{BN} = \frac{1}{X_{max} - X_{min}}$ and $b_{BN} = -\frac{X_{min}}{X_{max} - X_{min}}$.

The processed PSD features were then reshaped as a S×62×1×180 matrix, where S represented samples in datasets (i.e., 15(subjects)×3(sessions)×15(trials) samples in SEED and 15(subjects)×3(sessions)×24(trials) samples in SEED-IV), and 62 and 180 were the number of 62 channels and 180 epochs, respectively.

### *2.3. Organization of source domain and target domain*

**a) Organization of SEED dataset.** Processed PSD data of one randomly selected subject were used as data in target domain, while the rest of fourteen subjects were used as training data in source domain. Given that each subject had three experimental sessions and each session has fifteen trials, there were totally 14(subjects)×3(sessions)×15(trials) trials in source domain. As for target domain, three subjects were randomly selected and put into target domain, and one of them was used in turn in each round of DCNN training procedure.

In target domain, PSD features of three randomly selected trials (i.e., three trials with positive, neutral and negative emotions, respectively) in one experimental session were used as mapping targets and the rest twelve trials were used as testing data. In general, there were 1 (subjects)×3(sessions) experimental sessions in target domain, in which 1(subjects)×3(sessions)×3(trials) trials were mapping targets and 1(subjects)×3(sessions)×12(trials) trials were testing data.

Given that EEG signals have individual difference and instability in temporal dimension, each experimental session that was performed in a continuous time period was taken as an independent set of data. Therefore, there were totally 3(rounds)×14(subjects)×3(sessions) sets of training data and 3(rounds)×1(subjects)×3(sessions) sets of mapping targets and testing data. Thereinto, mapping targets and testing data belonged to a same experimental session.

**b) Organization of SEED-IV dataset.** The separation method of SEED-IV was same as SEED. Given that there were 15(subjects)×3(sessions)×24(trials) with four emotion categories in SEED-IV, 14(subjects)×3(sessions)×24(trials) trials were selected as training data in source domain and 1(subjects)×3(sessions) sessions were in target domain in each round of DCNN training procedure. Specifically, the mapping targets and testing data in target domain included 3(rounds)×1(subjects)×3(sessions)×4(trials) trials and 3(rounds)×1(subjects)×3(sessions)×20(trials) trials, respectively. In general, there were totally 3(rounds)×14(subjects)×3(sessions) sets of training data and 3(rounds)×1 (subjects)×3(sessions) sets of mapping targets and testing data in SEED-IV.

## 3. EEG domain adaption methodology

### *3.1. Domain adaption procedure*

The domain adaption framework includes three primary assignments: A) preprocessing the extracted features in SEED series datasets with ELBN for domain creation, B) mapping processed EEG features across individuals based on DCNN model and performing emotion recognition on DCNN outputs, and C) reading and analyzing mapping parameters with statistical analysis. The domain adaption concludes two linear mapping processes: ELBN and DCNN, which can be merged into one linear transformation. The procedure of domain adaption framework is illustrated in Fig. 3.

The experimental purposes and procedures of assignments above are described as follows. Assignment A is accomplished following the procedure in section II. It creates source domain and target domain for DCNN mapping procedure. In assignment B, DCNN is used to scale and translate data in the source domain to match that in the target domain without increasing or decreasing data. After repeated iteration and optimization operations of DCNN, the outputs are used to train classifiers that involves traditional machine learning and deep learning, which will be used to perform 5-fold validation and emotion recognition with testing data. Thereinto, 5-fold validation is to investigate the changes of EEG data in source domain after domain adaption, and emotion recognition with testing data is to test the effect of cross-subject mapping. In assignment C, the parameters of DCNN during mapping procedure are recorded. Given that ELBN and DCNN can be merged into a linear transformation, DCNN parameters are combined with ELBN parameters and then separated into scaling parameters and translation parameters. These combined parameters will be analyzed with statistical methods to figure out EEG emotion response mechanism.

### *3.2. DCNN model*

**a) DCNN model structure.** The DCNN model is constructed by a single depthwise convolutional layer with 62

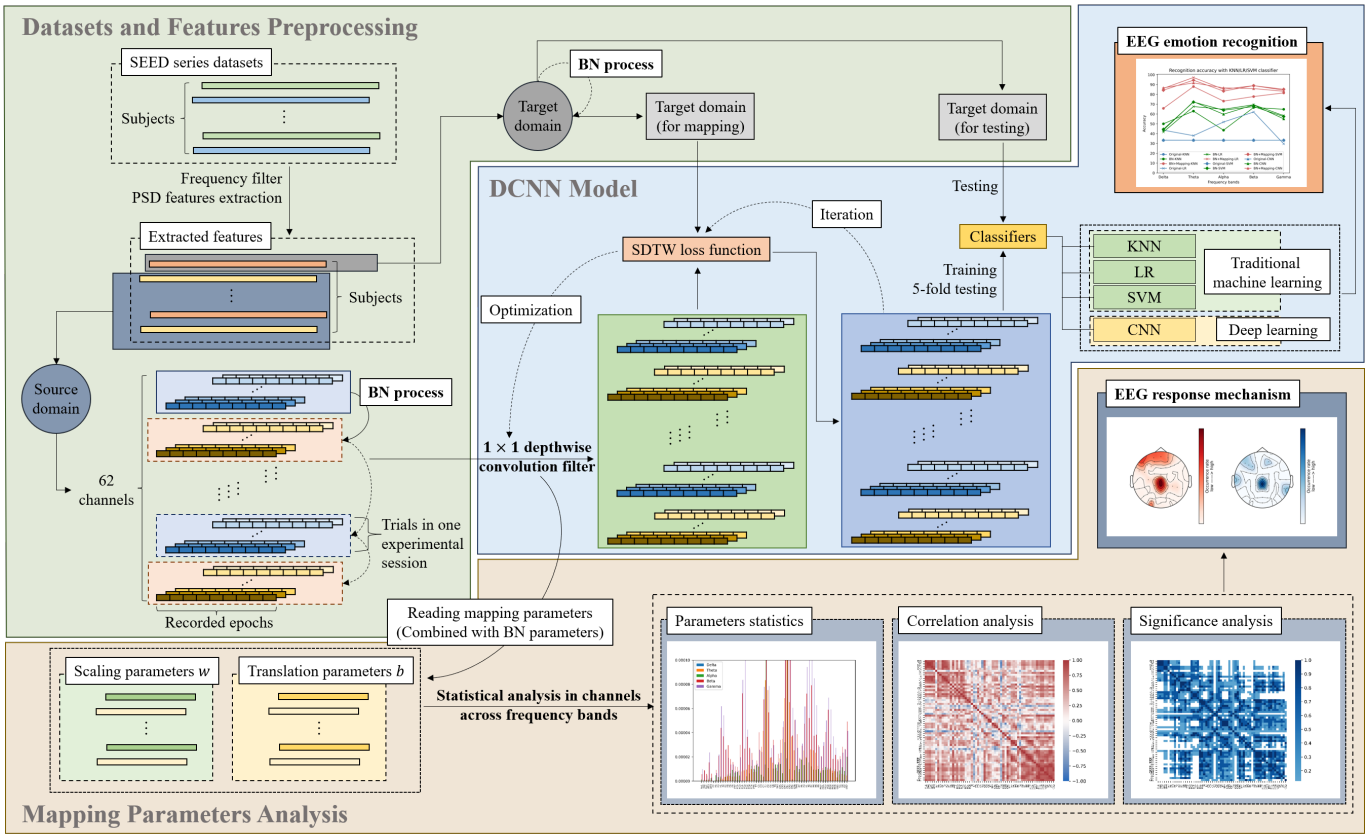


**Fig. 3.** Domain adaption framework.

group convolution kernels with $1 \times 1 kernel$ size and $1 \times 1$ stepwise. In each round of DCNN training, EEG inputs in one frequency band are reshaped as 62(channels)×1×180(epochs) so that 62 group convolution kernels can be used to map EEG data without mix the channel information (see Fig. 4). As each experimental session is an independent set, data in one experimental session are taken as a batch size. The calculation procedure is regarded as the second linear mapping process as:

$$X_{DCNN} = W_{DCNN} X_{BN} + B_{DCNN} \tag{3}$$

where $W_{DCNN}$ and $B_{DCNN}$ respectively represent the sets of scaling parameters $w_c$ and translation parameters $b_c$ $(1 \le c \le 62)$, $X_{BN}$ is the set of $X_{BN_k}$ in a batch size and $X_{DCNN}$ is the set of DCNN outputs. Owing to 62 group convolution kernels, data in each channel can share a scaling parameter $w_c$ and a translation parameter $b_c$ in a batch size. Meanwhile, considering the slight deviation between source domain and target domain, the initial value of w and b are set as 1 and 0, respectively.

**b) Loss function: $\gamma$-soft-DTW.** DTW is widely used in measuring the global similarity of time series [27]. The classic DTW algorithm is based on dynamic programming, which means that it gives a non-linear alignment between two time series. This produces a more intuitive similarity measure, allowing similar waveform to match even if they are located in different temporal periods. Therefore, given two time series $X = \{x_1, x_2, \cdots, x_m\}$ and $Y = \{y_1, y_2, \cdots, y_n\}$, the DTW distance is calculated by,

$$d(i,j) = \left(x_i - y_j\right)^2 \tag{4}$$

$$D(i,j) = d(i,j) + \min\left\{D(i-1,j), D(i,j-1), D(i-1,j-1)\right\} \tag{5}$$

$$\Delta(X,Y) = D(m,n) \tag{6}$$

where $i = 1, 2, \cdots, m$ and $j = 1, 2, \cdots, n$, and $D(i, j)$ is the accumulated distance value of time points between $x_i$ and $y_j$. $\Delta(X,Y)$ is distance between $X$ and $Y$ series. Let $\mathcal{A}_{m,n} \subset \{0,1\}^{m \times n}$ be possible binary alignment matrices that satisfy monotonicity, continuity and boundary conditions [28]. The DTW distance is then defined as:

$$DTW(X, Y) = \min_{A \in \mathcal{A}_{m,n}} \langle A, \Delta(X,Y) \rangle \tag{7}$$

To apply DTW as loss function in DCNN to calculate distance between training data and mapping targets, the differentiable $\gamma$-soft-DTW algorithm is used [29]. The generalized min operator with a smoothing parameter $\gamma$ in $\gamma$-soft-DTW is define as:

$$\min{}^{\gamma}\{a_1, \cdots, a_l\} := \begin{cases} \min_{k \le l} a_k, & \gamma = 0 \\ -\gamma log \sum_{k=1}^{l} e^{-a_k/\gamma}, & \gamma > 0 \end{cases} \tag{8}$$

With the operator, the $\gamma$-soft-DTW is defined as:

$$DTW_{\gamma}(X, Y) = \min_{A \in \mathcal{A}_{m,n}}{}^{\gamma} \{\langle A, \Delta(X,Y) \rangle\} \tag{9}$$

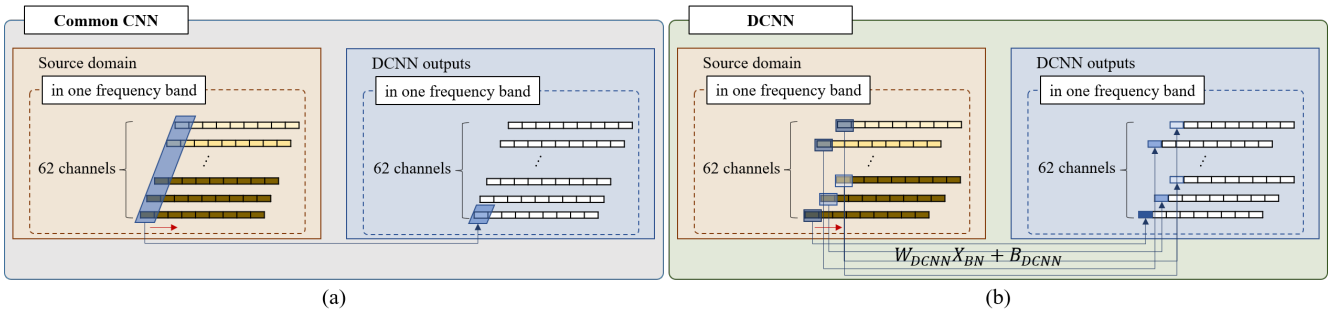


**Fig. 4.** The mapping process of common CNN and DCNN. (a) common CNN (b) DCNN.

**Table 1**
5-fold validation emotion recognition accuracies of SEED and SEED-IV. The positive values of the difference between original data group and other two groups are highlighted in red, and the positive values of the difference between groups with ELBN and groups with ELBN and DCNN are highlighted in green. All the negative difference values are highlighted in blue.

| Classifier | Band | Original(%) | | Original+ELBN(%) | | Original+ELBN+DCNN(%) | |
|---|---|---|---|---|---|---|---|
| | | SEED | SEED-IV | SEED | SEED-IV | SEED | SEED-IV |
| KNN | delta | 42.29 | 47.35 | 43.28(+0.79) | 61.38(+14.03) | 43.37(+0.88)(+0.09) | 70.52(+23.17)(+9.14) |
| | theta | 35.82 | 54.43 | 58.25(+22.43) | 64.12(+9.69) | 57.67(+21.85)(-0.58) | 73.48(+19.05)(+9.36) |
| | alpha | 34.18 | 49.44 | 46.88(+12.70) | 60.15(+10.71) | 49.63(+15.45)(+2.75) | 69.75(+20.31)(+9.60) |
| | beta | 42.12 | 45.33 | 55.87(+13.75) | 55.13(+9.80) | 57.86(+15.75)(+1.99) | 63.18(+17.85)(+8.05) |
| | gamma | 42.64 | 40.87 | 54.34(+11.70) | 49.27(+8.40) | 57.92(+15.28)(+3.58) | 52.07(+11.20)(+2.80) |
| LR | delta | 44.07 | 63.88 | 48.41(+4.34) | 71.99(+8.11) | 53.16(+9.08)(+4.75) | 74.60(+10.72)(+2.61) |
| | theta | 40.53 | 55.75 | 64.07(+23.54) | 71.30(+15.55) | 70.66(+30.13)(+6.59) | 74.87(+19.12)(+3.57) |
| | alpha | 35.87 | 63.26 | 61.96(+26.09) | 70.60(+7.34) | 61.55(+25.68)(-0.41) | 74.18(+10.92)(+3.58) |
| | beta | 40.53 | 51.15 | 66.61(+26.08) | 71.03(+19.88) | 66.38(+25.85)(-0.23) | 72.09(+20.94)(+1.06) |
| | gamma | 50.58 | 56.31 | 64.18(+13.60) | 67.23(+10.92) | 65.20(+14.62)(+1.02) | 67.74(+11.43)(+0.51) |
| SVM | delta | 43.02 | 59.10 | 48.10(+5.08) | 67.30(+8.20) | 52.56(+9.54)(+4.46) | 72.09(+12.99)(+4.79) |
| | theta | 44.71 | 57.61 | 59.74+15.03 | 66.61(+9.00) | 68.82(+24.11)(+9.08) | 72.33(+14.72)(+5.72) |
| | alpha | 45.50 | 53.57 | 58.36(+12.86) | 65.91(+12.34) | 60.30(+14.80)(+1.94) | 70.96(+17.39)(+5.05) |
| | beta | 45.71 | 53.41 | 63.76(+18.05) | 64.76(+11.35) | 65.11(+19.40)(+1.36) | 68.74(+15.33)(+3.98) |
| | gamma | 48.20 | 55.85 | 61.43(+13.23) | 62.87(+7.02) | 64.83(+16.63)(+3.41) | 65.60(+9.75)(+2.73) |
| CNN | delta | 33.33 | 76.95 | 68.13(+34.80) | 76.09(-0.86) | 65.42(+32.09)(-2.71) | 75.79(-1.16)(-0.30) |
| | theta | 33.32 | 75.90 | 76.83(+43.51) | 75.10(-0.80) | 77.71(+44.39)(+0.88) | 76.16(+0.26)(+1.06) |
| | alpha | 33.26 | 75.57 | 73.08(+39.82) | 73.76(-1.80) | 69.56(+36.30)(-3.52) | 75.36(-0.21)(+1.60) |
| | beta | 33.39 | 76.95 | 74.78(+41.39) | 74.42(-2.53) | 73.73(+40.33)(-1.05) | 74.61(-2.34)(+0.19) |
| | gamma | 33.53 | 76.81 | 71.50(+37.97) | 74.24(-2.57) | 72.13(+38.60)(+0.63) | 73.82(-2.99)(-0.42) |

### *3.3. Domain adaption procedure and emotion recognition*

In section 2, processed EEG features in source domain (i.e., training data) and target domain (i.e., mapping target and testing data) are divided into independent sets. In each round of DCNN training procedure, one set of mapping targets will be selected as the labels of one set of training data with corresponding emotions (e.g., positive PSD features in source domain are mapped to the positive PSD features of mapping targets). At each iteration, $\gamma$-soft-DTW function calculates and returns the sDTW value for mapping parameters optimization and similarity improvement direction from source domain to mapping targets. After a thousand times of iteration and optimization operations in DCNN, the outputs will be then used to train classifiers (i.e., k-nearest neighbor (KNN), logistic regression (LR), support vector machine (SVM), and CNN. These trained classifiers will be evaluated by 5-fold validation and applied to testing data in the same set of mapping targets. Therefore, there are totally 3(subjects)×3(sessions)×42(sets of training data)×5(frequency bands) rounds of DCNN mapping procedure.

### *3.4. Mapping parameters analysis*

**a) Purposes.** The scaling and translation parameters of DCNN are analyzed with statistical methods to find the EEG emotion response mechanism across channels and frequency bands. EEG data in source domain are mapped to the data of mapping targets through two linear mapping processes (i.e., ELBN and DCNN procedure), which can be summarized as a linear mapping process as,

$$\begin{aligned} X_{DCNN} &= W_{DCNN}\left(w_{BN}\left\{X_k\right\} + b_{BN}\right) + B_{DCNN} \\ &= W\left\{X_k\right\} + B \end{aligned} \tag{10}$$

where $\{X_k\}$ denotes the set of PSD inputs in an experimental session, $W = W_{DCNN}w_{BN}$ and $B = W_{DCNN}b_{BN} + B_{DCNN}$.

Given a mapping target in DCNN training procedure, the whole mapping procedure is a linear transformation where each channel and frequency band have an exclusive scaling parameter in $W$ and translation parameter in $B$ in each round of mapping procedure (see Fig. 5). By mapping different EEG data of training data to one common mapping target, the difference between training data can be found through the values of mapping

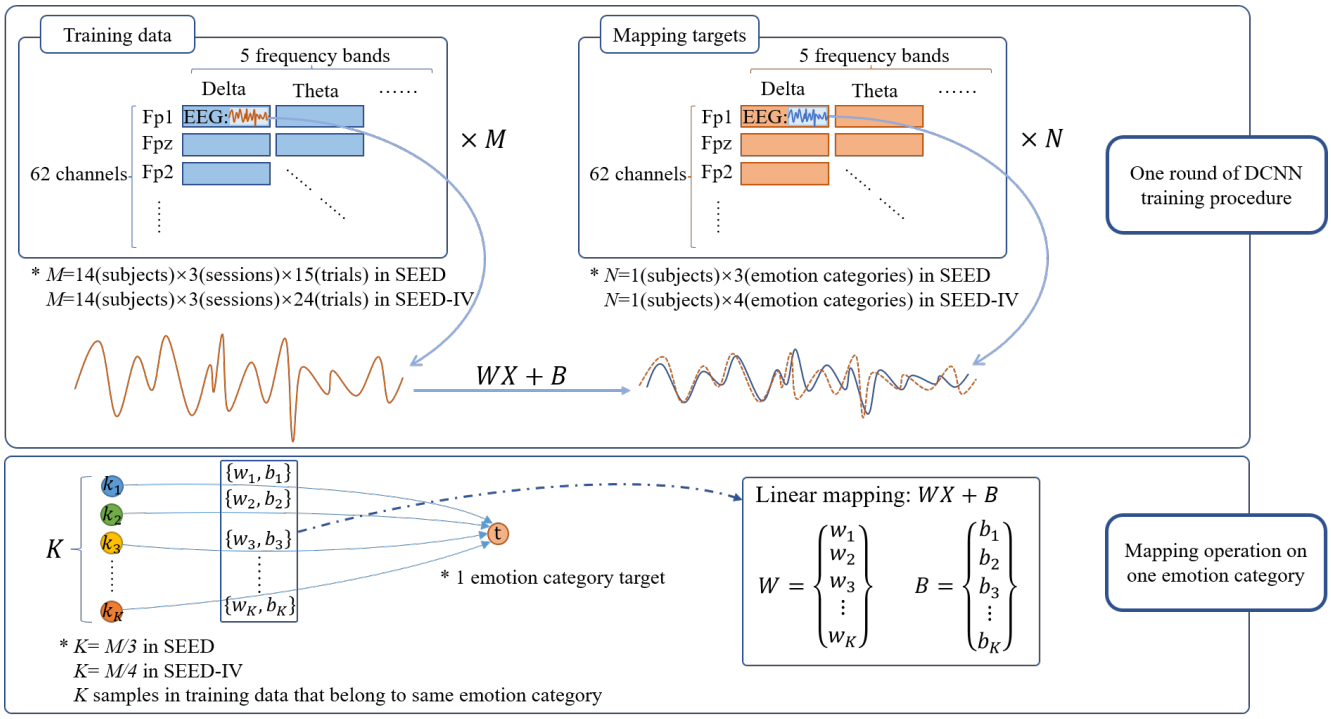


**Fig. 5.** Application of mapping parameters.

parameters. For example, given three samples $k_1, k_2, k_3$ that belong to same emotion category in training data and a mapping target $t$ in mapping targets, there are three pairs of mapping parameters $\{w_1, b_1\}$, $\{w_2, b_2\}$, $\{w_3, b_3\}$ corresponding to three samples. The mapping procedure can be described as:

$$\begin{bmatrix} k_1 \\ k_2 \\ k_3 \end{bmatrix} \cdot \begin{bmatrix} w_1 \\ w_2 \\ w_3 \end{bmatrix} + \begin{bmatrix} b_1 \\ b_2 \\ b_3 \end{bmatrix} = \begin{bmatrix} t \\ t \\ t \end{bmatrix} \tag{11}$$

The greater similarity between samples exists, the smaller difference between mapping parameters can be found. That is, the values of mapping parameters can be used to measure the difference of EEG samples. Furthermore, according to the one-to-one correspondence between mapping parameters and channels as well as frequency bands, mapping parameters can be regarded as EEG features to figure out the EEG emotion response mechanism based on channels and frequency bands.

**b) Statistical analysis processes.** The statistical analysis on parameters W and B in channels across frequency bands includes three parts: 1) parameter numerical statistics, 2) correlation analysis, and 3) nonparametric significance testing. In parameter numerical statistics, the parameters in the same channel and frequency band are averaged firstly and then compared across channels and frequency bands to explore their distributions. In correlation analysis and nonparametric significance testing, parameters in the same frequency bands of one experimental session are firstly averaged. The averaged data in each channel and frequency band are used as averaged scaling and translation parameters in one source domain adaption that maps training data to mapping targets. Corresponding to 3(rounds)×1(subjects)×3(sessions) sets of mapping targets, there are 18 averaged parameters (i.e., 9 scaling averaged parameters and 9 averaged translation parameters respectively) in one channel under one frequency band in each dataset. Statistical analysis is performed on the averaged data of every two channels of the same frequency band. Specifically, Spearman's rank correlation [30] is used in correlation analysis to compute the correlation, and Mann-Whitney U test [31] is used in nonparametric significance testing to compute the pairwise p-value. It's defined that the pairwise channels are significantly different when their p-values are no higher than 0.05.

## 4. Results

### 4.1. Emotion recognition results

The 5-fold validation emotion recognition results of SEED and SEED-IV are shown in Table 1. The experimental groups include original PSD features, PSD features processed with ELBN, and PSD features processed with ELBN and DCNN mapping. Compared with the original data group, the ELBN approach can improve most of the recognition accuracies by 0.79%-43.51% in all the five frequency bands when using the employed classifiers. The DCNN mapping process can further improve most of recognition results in both SEED and SEED-IV on the basic of ELBN by 0.09%-9.60%. In particular, the highest increment with ELBN and DCNN in SEED is up to 44.39% in theta frequency band when using the CNN classifier, while the highest number in SEED-IV is up to 23.17% in delta frequency band when using KNN. It indicates that the differences of EEG data across individuals and experimental sessions (i.e., the changing pattern of EEG in temporal dimension) can be effectively diminished by mapping EEG data to a mutual target with linear transformation. Furthermore,

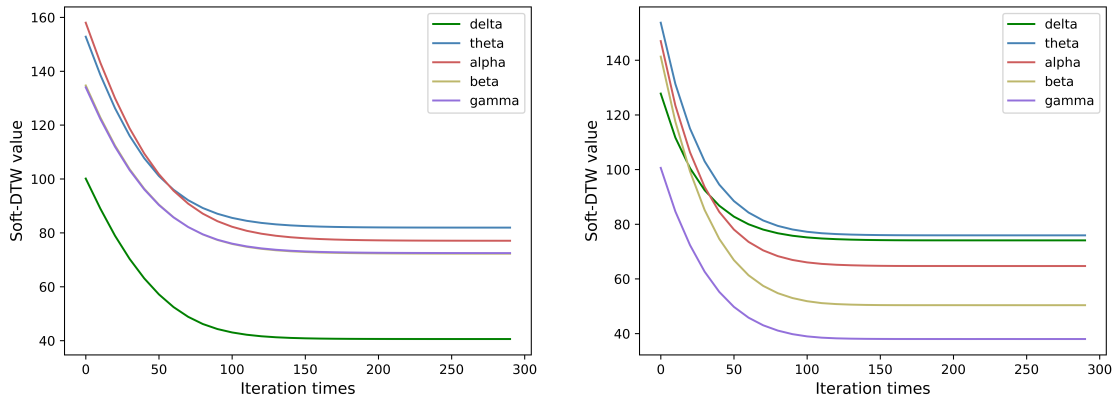


(a) Loss in SEED dataset.

(b) Loss in SEED-IV dataset.

**Fig. 6.** The averaged $\gamma$-soft-DTW loss curves in five frequency bands.

**Table 2**
Emotion recognition accuracies on testing data of SEED and SEED-IV. The positive values of the difference between original data group and other two groups are highlighted in red, and the positive values of the difference between groups with ELBN and groups with ELBN and DCNN are highlighted in green. All the negative difference values are highlighted in blue.

| Classifier | Band | Original(%) | | Original+ELBN(%) | | Original+ELBN+DCNN(%) | |
|---|---|---|---|---|---|---|---|
| | | SEED | SEED-IV | SEED | SEED-IV | SEED | SEED-IV |
| KNN | delta | 33.33 | 25.00 | 50.00(+16.67) | 60.00(+35.00) | 65.74(+32.41)(+15.74) | 73.89(+48.89)(+13.89) |
| | theta | 33.33 | 25.00 | 62.96(+29.63) | 59.45(+34.45) | 87.96(+54.63)(+25.00) | 69.44(+44.44)(+9.99) |
| | alpha | 33.33 | 25.00 | 43.52(+10.88) | 60.55(+35.55) | 73.15(+39.82)(+29.63) | 75.00(+50.00)(+14.45) |
| | beta | 33.33 | 25.00 | 66.67(+33.34) | 51.11(+26.11) | 77.78(+44.45)(+11.11) | 60.00(+35.00)(+8.89) |
| | gamma | 33.33 | 25.00 | 64.82(+31.49) | 48.89(+23.89) | 81.48(+48.15)(+16.66) | 55.00(+30.00)(+6.11) |
| LR | delta | 43.52 | 56.67 | 41.67(-1.85) | 70.56(+13.89) | 86.11(+42.59)(+44.44) | 80.00(+23.33)(+9.44) |
| | theta | 37.96 | 49.44 | 67.59(+29.63) | 69.44(+20.00) | 97.22(+59.26)(+29.63) | 74.44(+25.00)(+5.00) |
| | alpha | 51.85 | 51.11 | 64.82(+12.97) | 70.56(+19.45) | 85.19(+33.34)(+20.37) | 77.22(+26.11)(+6.66) |
| | beta | 62.04 | 43.33 | 69.44(+7.41) | 65.00(+21.67) | 88.89(+26.85)(+19.45) | 72.22(+28.89)(+7.22) |
| | gamma | 29.63 | 50.00 | 58.33(+28.70) | 61.67(+11.67) | 84.26(+54.63)(+25.93) | 72.22(+22.22)(+10.55) |
| SVM | delta | 33.33 | 25.00 | 44.44(+11.11) | 68.89(+43.89) | 84.26(+50.93)(+39.82) | 71.67(+46.67)(+2.78) |
| | theta | 33.33 | 25.00 | 72.22(+38.89) | 59.44(+34.44) | 94.44(+61.11)(+22.22) | 70.00(+45.00)(+10.56) |
| | alpha | 33.33 | 25.00 | 63.89(+30.56) | 68.89(+43.89) | 83.33(+50.00)(+19.44) | 72.22(+47.22)(+3.33) |
| | beta | 33.33 | 25.00 | 67.59(+34.26) | 58.33(+33.33) | 88.89(+55.56)(+21.30) | 70.00(+45.00)(+11.67) |
| | gamma | 33.33 | 25.00 | 57.41(+24.08) | 56.67(+31.67) | 85.18(+51.85)(+27.77) | 69.44(+44.44)(+12.77) |
| CNN | delta | 33.39 | 73.24 | 43.64(+10.25) | 71.02(-2.22) | 86.64(+53.25)(+43.00) | 79.50(+6.26)(+8.48) |
| | theta | 33.33 | 72.98 | 72.59(+39.26) | 69.11(-3.87) | 91.70(+58.37)(+19.11) | 77.96(+4.98)(+8.85) |
| | alpha | 33.33 | 72.26 | 59.78(+26.45) | 68.68(-3.58) | 86.64(+53.31)(+26.86) | 77.80(+5.54)(+9.12) |
| | beta | 33.33 | 69.93 | 69.26(+35.93) | 68.65(-1.28) | 85.90(+52.57)(+16.64) | 75.71(+5.78)(+7.06) |
| | gamma | 33.33 | 70.52 | 55.06(+21.73) | 68.52(-2.00) | 83.15(+49.82)(+28.09) | 74.08(+3.56)(+5.56) |

compared with the experimental-session-independent normalization, DCNN can link experimental sessions in the source domain and experimental sessions of mapping targets to achieve a more purposive and sophisticated mapping effect by means of iteration and optimization operations of the neural network. However, comparing results in Table 1, the increments in SEED are better than those in SEED-IV, which may be caused by the more emotion categories and more zero paddings in SEED-IV.

The emotion recognition results on the testing data of SEED and SEED-IV are shown in Table 2. The recognition results of the original data group obviously show the gap between individuals. Classifiers trained with subjects in the source domain have poor emotion recognition performance on subjects in the target domain. Compared with the original data group, the ELBN approach can improve most of the recognition results in both SEED and SEED-IV, and the results of ELBN can be further improved by incorporating DCNN mapping. The recognition accuracies are all increased across frequency bands and classifiers compared with the original data group. As shown in Table 2, the highest recognition accuracies with ELBN and DCNN in SEED and SEED-IV are 97.22% and 80.00%, respectively. The highest increment in SEED is up to 61.11% when using SVM classifier in theta frequency band, while that in SEED-IV is up to 50.00% when using KNN classifier in alpha frequency band. Furthermore, compared with the results in Table 1, the influence of DCNN mapping process is better in Table 2. As shown in Table 2, the increment in SEED is up to 39.82% after adding DCNN mapping, but the increment of SEED is only up to 9.08% in Table 1. Similarly, in SEED-IV, the increment with adding DCNN mapping is up to 13.89% in Table 2, while that in Table 1 is only up to 9.60%. It indicates that the DCNN mapping works more effectively to dimmish the individual dif-

**Table 3**
The number of channels in which each channel has significant difference with more than 25%, 50% and 75% of other 61 channels.

| Dataset | SEED | | | | | | SEED-IV | | | | | |
|---|---|---|---|---|---|---|---|---|---|---|---|---|
| Mapping Parameter | Scaling parameter | | | Translation parameter | | | Scaling parameter | | | Translation parameter | | |
| Percentage of significantly different channels | >25% | >50% | >75% | >25% | >50% | >75% | >25% | >50% | >75% | >25% | >50% | >75% |
| Number of channels | 61 | 60 | 22 | 62 | 34 | 12 | 62 | 53 | 25 | 8 | 2 | 1 |

**Table 4**
Comparison results on SEED and SEED-IV datasets. The highest accuracies on SEED and SEED-IV datasets across methods are highlighted in bold, respectively.

| Author | Published year | Method | Dataset | Highest accuracy (%) |
|---|---|---|---|---|
| Chen et al. [32] | 2021 | Multi-source marginal distribution adaptation (MS-MDA) | SEED | 89.63 |
| | | | SEED-IV | 59.34 |
| Li et al. [33] | 2021 | Self-organized graph neural network (SOGNN) | SEED | 86.81 |
| | | | SEED-IV | 75.27 |
| Li et al. [34] | 2022 | Dynamic domain adaptation (DDA) | SEED | 91.08 |
| | | | SEED-IV | **81.58** |
| Peng et al. [35] | 2022 | Joint EEG feature transfer and semisupervised cross-subject emotion recognition model | SEED | 84.69 |
| | | | SEED-IV | 78.85 |
| Magdiel and Gibran [36] | 2023 | Multi-source feature alignment and label rectification (MFA-LR) | SEED | 89.11 |
| | | | SEED-IV | 74.99 |
| This study | - | Linear domain adaption | SEED | **97.22** |
| | | | SEED-IV | 80.00 |

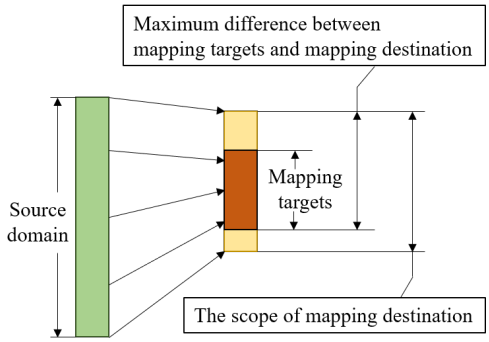


**Fig. 7.** Illustration of DCNN mapping destination.

ference between source domain and target domain, though it can also improve 5-fold validation results in source domain. It's because the direction of DCNN mapping procedure is to reduce sDTW values between training data in source domain and mapping targets in target domain so that the similarity between them can be augmented definitely. The $\gamma$-soft-DTW loss curves of five frequency bands that are averaged in channels are shown in Fig. 6. Although the mapping direction is common in source domain, the scope of mapping destination is wider, leading to more individual difference in mapped data of source domain (see Fig. 7).

### *4.2. Statistical analysis results*

**a) Parameter numerical statistics.** The parameter numerical statistics results of scaling parameters W and translation parameters B are shown in Fig. 8, respectively. Firstly, given that the whole mapping procedure is a linear transformation (see Eq. (9)) that W and B transform the EEG data values to diminish difference between individuals (see Fig. 6) without changing their waveforms, it can be inferred that the waveforms between individual EEG data are pretty similar but the values of them are variant. This could be resulted from the individual difference, instability of EEG patterns in temporal dimension and experimental error in experimental sessions [8],[26]. This finding could reveal how the EEG difference is reflected on practical recorded EEG data, in which the global values of EEG data are directly influenced but the waveforms in a limited temporal range are relatively stable. Furthermore, as shown in Fig. 8, the parameter distribution is hierarchical in five frequency bands and the parameters in channels from same frequency band can be regarded as a relatively integration. The boundaries between frequency bands are obviously existing and the EEG data across channels fluctuate within boundaries. Meanwhile, parameters from parietal lobe are prone to higher scaling values and lower translation values in both SEED and SEED-IV. That is, the scale extent of EEG data from parietal lobe is significantly lesser than other brain cortex regions. Thereinto, outlier data of $W$ parameters occur at the region centered in Cz and CPz channels, which is the center of parietal lobe. This could be attributed to the use of EEG cap where parietal lobe (especially the positions of Cz and CPz) are prone to be firstly located with higher location accuracy, while the locations of other channels on cap are easier to move because of the deformation of EEG cap and difference of subjects' head shape. This can result in more experimental errors in channels, which makes difference greater between experimental sessions and requires more scaling operations. The integration of channels can be enhanced if the experimental errors above can be diminished.

**b) Correlation analysis.** Fig. 9 and Fig. 10 show the correlation analysis results in SEED and SEED-IV, respectively. The pairwise correlation of channels shows that there is obviously positive correlation in most channels. This correlation is existing across frequency bands and evenly distributed in global brain cortex region, which is in accord with the previous conclusion that EEG data in 62 channels are a unity when in emotion response. Furthermore, given that there are three emotion categories in SEED and four in SEED-IV, the overall correlation in SEED-IV is stronger than that in SEED in all the five frequency bands. The range of positive correlation in channels in SEED-IV is greater as well. It indicates that the experimental emotion complexity (i.e., emotion categories) can influence the

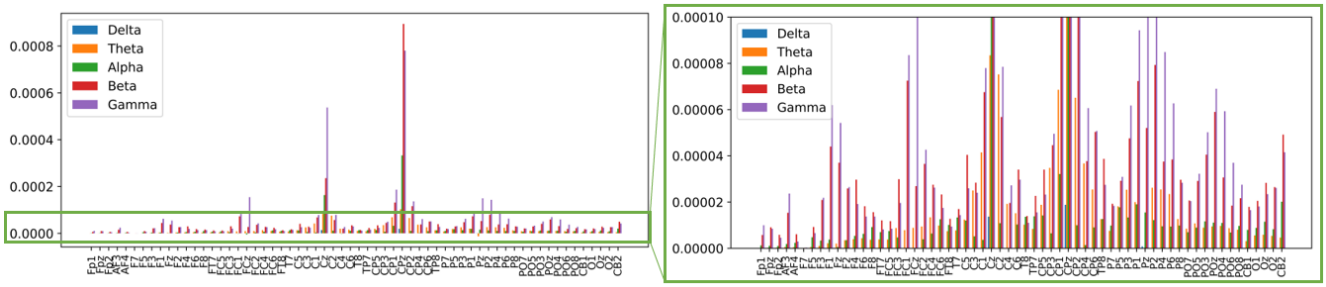


(a) Scaling parameter numerical statistics of SEED.

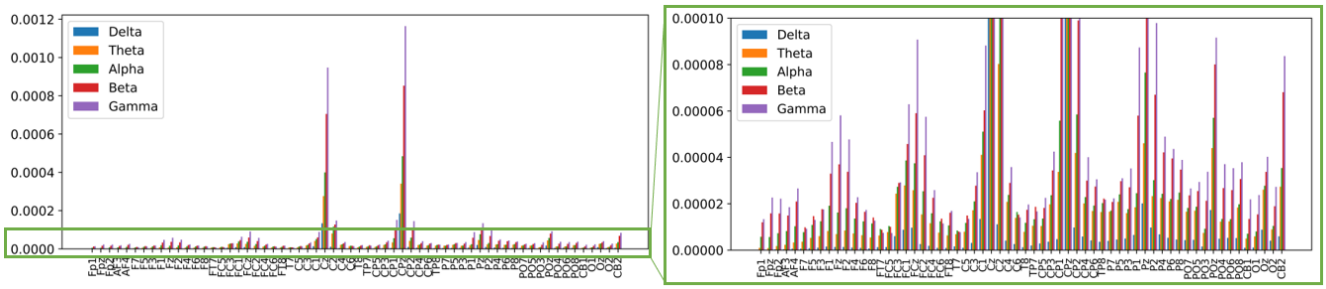


(b) Scaling parameter numerical statistics of SEED-IV.

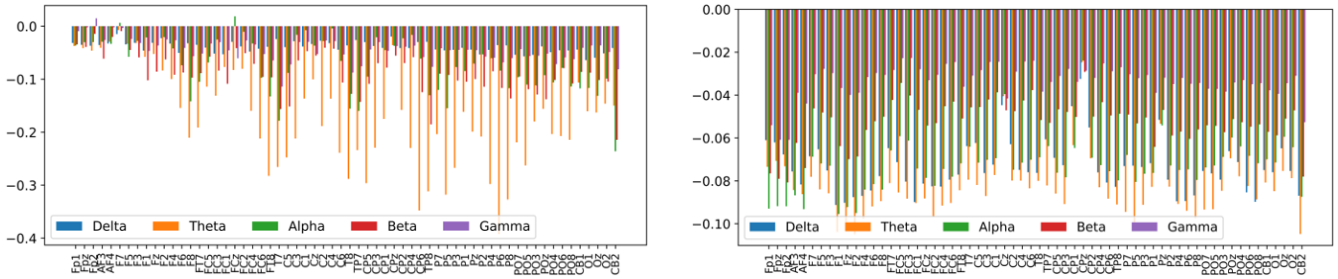


(c) Translation parameter numerical statistics of SEED (left) and SEED-IV (right).

**Fig. 8.** Parameter numerical statistics in SEED and SEED-IV dataset. The x-axis represents the 62 channels and the y-axis represents the value of parameters.

correlation of channels. Higher degree in emotion complexity contributes to strengthened integration of channels. However, the effect of such an influence should be further discussed. On the one hand, the integration of channels implies that the global EEG signals can be obtained with fewer channels. On the other hand, the global features extraction (e.g., convolutional layers of CNN) maybe impacted as less differences between brain cortex regions are preserved with higher emotion complexity, which could be a difficulty for multi-emotion recognition.

**c) Nonparametric significance testing.** The nonparametric significance testing is performed on mapping parameters of SEED and SEED-IV, and the results are shown in Fig. 11 and Fig. 12, respectively. The number of channels that have significant difference with more than 25%, 50% and 75% of other channels is recorded in Table 4. It can be found that most of channels in different brain regions have no significant difference across frequency bands, which means that most channels are interconnected without the limitation of brain regions in emotion responses. Specifically, as shown in Table 4, nearly all channels have significant difference with more than 25% of other channels, but less than a half of channels are significantly different with other channels when the percentage is more than 75%. It shows that the difference between channels is limited especially when the scope covers the whole brain regions, which further proves the integration of channels. However, as shown in Fig. 12 and Fig. 12, the interconnection doesn't appear in frequency bands. The p-value distributions in frequency bands are obviously different, which is consistent with the hierarchy characteristics in parameter numerical statistics analysis before.

Furthermore, as there are a few channels that have significant difference with most of the others in some of frequency bands, each channel that has significant difference with over 75% of other channels in each frequency band is recorded. The occurrence numbers of these channels in SEED and SEED-IV is counted and transformed as occurrence rate by dividing 10 (i.e., 2(datasets)×5(frequency bands)). The occurrence rates calculated by $W$ and $B$ are illustrated in Fig. 13. As shown in Fig. 13, the regions of high occurrence rate are concentrated on parietal lobe and parts of frontal lobe/occipital lobe, which are recognized as the emotion-insensitive brain cortex region in previous studies [8],[22]. It indicates that emotion sensitiveness of brain cortex region can influence the correlation between channels. Channels in relatively insensitive regions are more likely to have weaker correlations with other channels. However, it

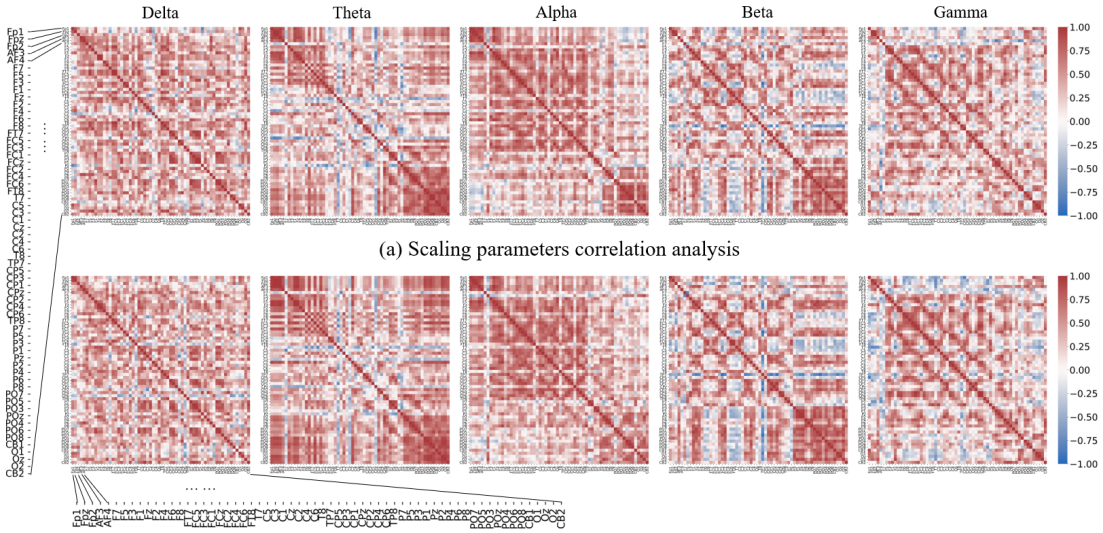


(a) Scaling parameters correlation analysis

(b) Translation parameters correlation analysis

**Fig. 9.** Parameter numerical statistics in SEED and SEED-IV dataset. The x-axis represents the 62 channels and the y-axis represents the value of parameters.

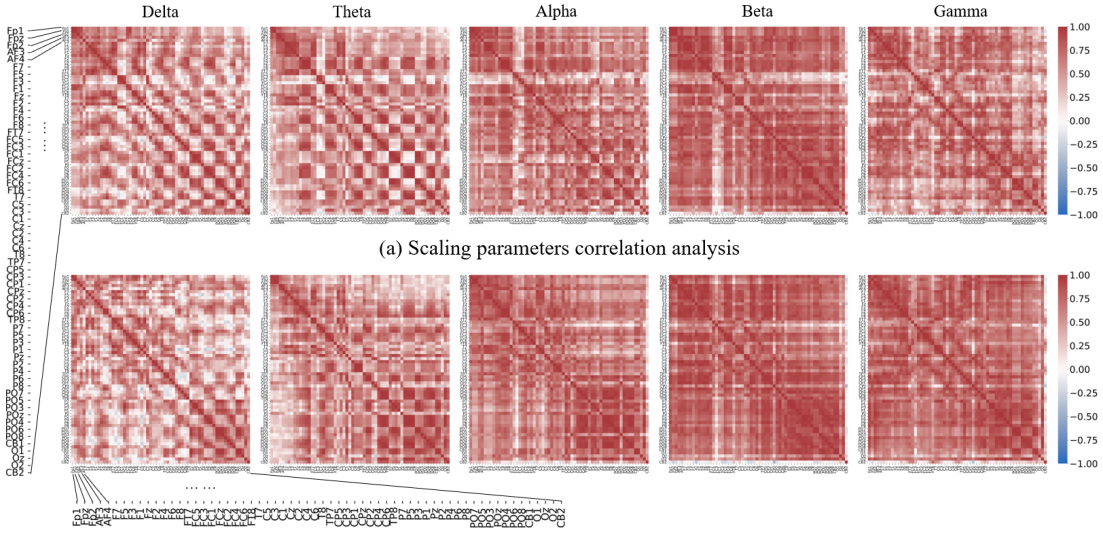


(a) Scaling parameters correlation analysis

(b) Translation parameters correlation analysis

**Fig. 10.** Parameter numerical statistics in SEED and SEED-IV dataset. The x-axis represents the 62 channels and the y-axis represents the value of parameters.

should be noticed that this weak correlation happens in a few parts of frequency bands with relatively small probabilities and doesn't significantly influence the general integration of channels.

### *4.3. Comparative analysis*

To further evaluate the performance of the proposed linear domain adaption method, related methods (especially for transfer learning) that perform cross-subject EEG-based emotion recognition on the SEED and SEED-IV datasets are involved for comparative analysis. As shown in Table 4, these related methods realized good cross-subject emotion recognition performance by using deep learning networks and transfer learning. The highest recognition accuracies of related methods on SEED and SEED-IV datasets are 91.08% and 81.58% respectively, while the method in this study attains recognition accuracies of 97.22% and 80.00% for the same datasets. It shows that the proposed method can achieve comparable and even much higher cross-subject emotion recognition accuracy. Furthermore, as the related methods in Table 4 are based on neural network with deep layers, it needs more computational costs when comparing with the proposed method that integrates single neural network layer with shallow machine learning. The interpretability problem also appears in the deep neural network model above, leading to the fact that unparsable model parameters hinder the further investigation of models and EEG emotion response mechanisms. In contrast, parameters in the linear domain adaptation model can be completely parsed and utilized as features to investigate the underlying EEG mechanisms due to the simplified model structure. In general, com-

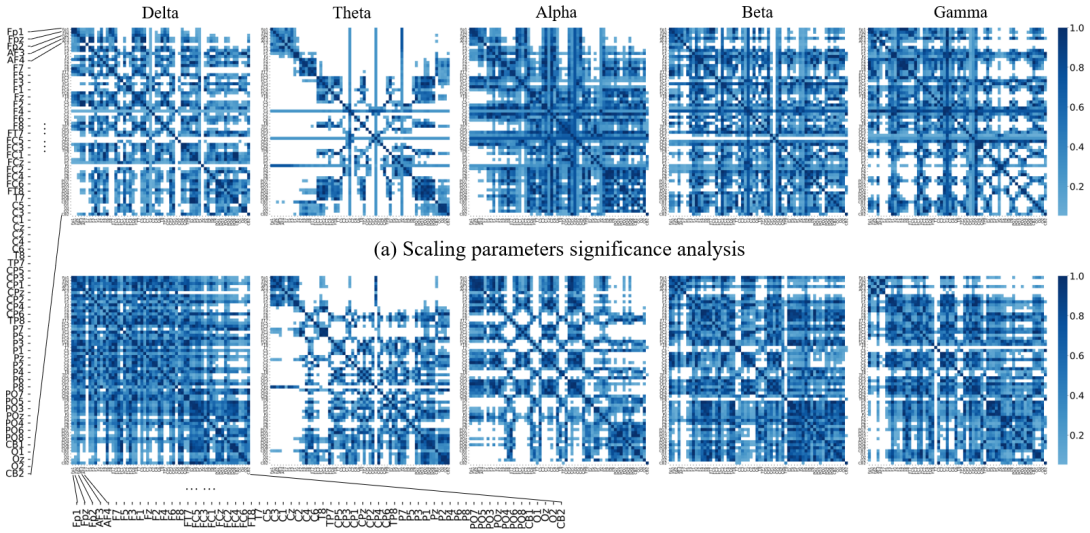


(a) Scaling parameters significance analysis

(b) Translation parameters significance analysis

**Fig. 11.** Parameter numerical statistics in SEED and SEED-IV dataset. The x-axis represents the 62 channels and the y-axis represents the value of parameters.

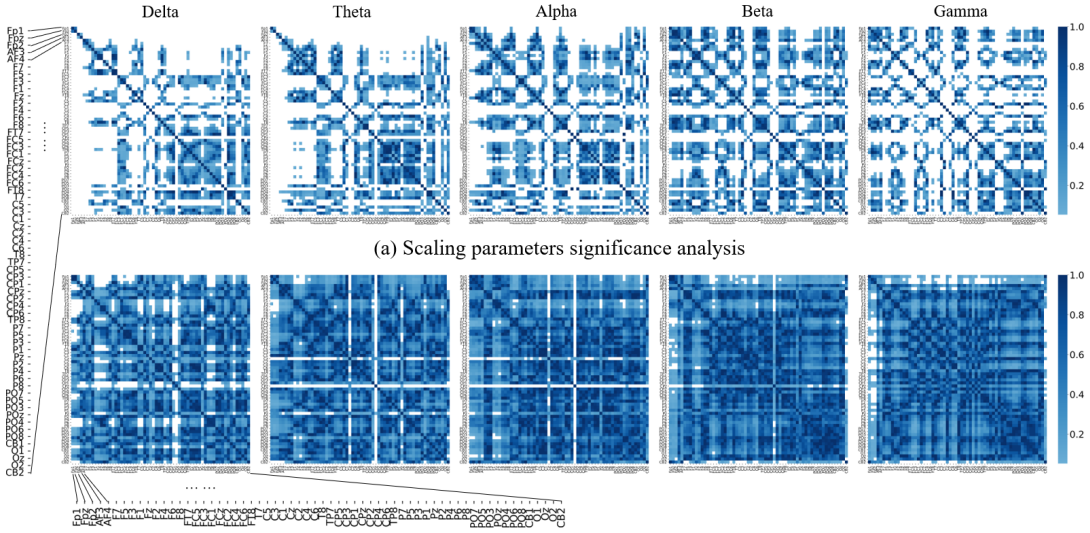


(a) Scaling parameters significance analysis

(b) Translation parameters significance analysis

**Fig. 12.** Parameter numerical statistics in SEED and SEED-IV dataset. The x-axis represents the 62 channels and the y-axis represents the value of parameters.

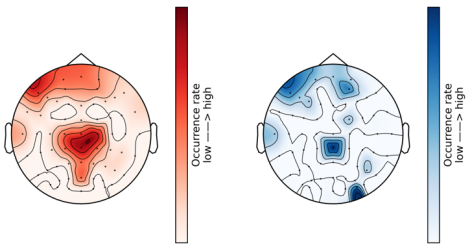


**Fig. 13.** Occurrence rate of channel-unrelated channels based on mapping parameters.

pared with other related methods, the proposed method in this study can make fully use of the network model to achieve high EEG-based cross-subject emotion recognition accuracy as well as EEG emotion mechanisms investigation.

## 5. Discussion

### *5.1. Brain cortex regions and channels integration*

The functions of brain cortex regions should be further investigated and determined in affective computing as the channel integration is out of regions constraint. Previous studies divide brain cortex into different functional regions [22],[37], such as the orbital frontal cortex, ventral medial prefrontal cortex, and amygdala [38],[39]. Channels located at different brain cortex regions contribute differently to emotion recognition [40],[41] and hence selecting channels from the right brain cortex regions is helpful for improving emotion recognition accuracy [8],[22],[42]. However, in statistical analysis results, it is found

that channels can be regarded as an integrated unity that breaks the boundary between different brain cortex regions. Nonparametric significance testing results show that brain cortex regions associated with emotions have different performances in channel correlation. However, the occurrence rate of such difference is still in low degree. In general, it is believed that difference exists between different brain cortex regions in emotion response studies. However, given that channel locations could move because of the deformation of EEG cap and the difference in subjects' head shape when using EEG cap to collect EEG signals, the range of brain cortex regions is not strictly fixed in experiments. This undefined brain cortex regions could intervene in the expression of EEG signals collected from different regions, which may further lead to the magnification of difference between brain cortex regions. Therefore, it should be further investigated how the position offset of channels influences the EEG signals collection and brain cortex region functions as well as the influence extent, and whether the differences between brain cortex regions are overestimated.

### *5.2. Hierarchy characteristic of frequency bands*

The hierarchy characteristic of frequency bands has no perceptible influence on emotion recognition since there is no significant difference in the recognition accuracy of different frequency bands. According to the results in Tables 1-2, there is no significant difference in the recognition accuracy of different frequency bands, indicating that hierarchy characteristic of frequency bands does not affect emotion recognition significantly. Consistent with previous studies, it has been shown that EEG signals in diverse frequency bands could be associated with specific human activities [43],[44]. For example, alpha band is related to the state when a person is relaxed and conscious, while beta band is related to the state that human mind is active and highly concentrated [45]. Moreover, it was found that emotion EEG signals are more active in the low-frequency band than that in the high-frequency band, and a wider distribution and higher intensity occur in negative emotion responses than in positive emotion [46]. However, in the recognition results of different frequency bands in Tables 1-2, there is no significant difference in frequency bands across classifiers. The recognition performances have little identifiable difference in different frequency bands across classifiers and datasets. It seems that the difference of frequency bands cannot be well reflected in emotion recognition results. It may be because that the EEG data of different frequency bands share the same original source data and the effective information is distributed unevenly in different frequency bands. Hence, for improving EEG emotion recognition, dividing EEG signals into several frequency bands to attain more frequency features is more useful than taking EEG signals from one specific frequency band. This view can be supported by previous studies which conclude that using the organization of all frequency bands could achieve better emotion recognition accuracy than using a single band [22].

### *5.3. Potential application*

Beyond previous CNN based emotion recognition methods, which prefer to focusing on EEG data of some specific research areas, the proposed methods (i.e., ELBN and DCNN mapping) can transfer EEG data from one domain into another. As shown in the recognition accuracy of Tables 1-2, the mapping process is able to map the EEG features from one subject to another, reinforcing the similarity between subjects' EEG data and improving emotion recognition across subjects. Based on the characteristics of the proposed methods, this study sees several ways in which the method could be used to improve emotion recognition. Firstly, since the individual differences or experimental errors could lead to differences in separate datasets, one key implication of the proposed method is to integrate diverse EEG datasets and extend their potential use cases. Specifically, the external EEG data from other subjects can be mapped to a specific person as his/her training data for emotion recognition classifiers, which can change the situation that one subject should participate in experiments many times to collect enough EEG data for training classifiers. That is, EEG data of a specific subject are expended by transferring other EEG data. Moreover, this expansion ability of mapping process can also be used in mapping EEG across different research areas. For example, the emotional EEG signals elicited in daily life can be used to recognize driving emotion [47], which is helpful for building driving assistance systems. Additionally, the EEG signals elicited in different scenarios can be intercommunicated and the content of them can be enriched by each other. The applicable categories of EEG conclude not only emotions but also other human activities, such as distraction EEG signals [48].

### *5.4. Limitations and future work*

The main limitations and future work of this study can be summarized as follows. Firstly, in the features processing procedure, features in some of trials that less than 180 epochs are filled with zeros. The unified format of EEG features is beneficial to data application in classifiers, and zero paddings will be ignored in feature identified. However, zero paddings will influence the results of ELBN outputs. Though these outputs will be rectified in the following DCNN mapping processes, whether EEG data without zero padding have better classification results is still need to be investigated in the future. Secondly, the scaling parameters $W$ and translation parameters $B$ are both analyzed in statistical analysis. In most cases, these two kinds of parameters are distributed similarly. However, in parameter numerical statistics results shown in Fig. 8 and Fig. 9, $W$ and $B$ show different distribution in frequency bands, which makes it difficult to determine how frequency bands work in human emotion responses. In future work, the variant parameters should be further decreased to ensure the states of frequency bands in emotion responses. Finally, there are only four EEG emotion categories used in this study. However, human emotion categories are much more than four. To further validate the conclusions of the experimental analysis, more emotion categories should be involved in future study. In the meanwhile, more sound and representative emotion measurements can be used for EEG emotion analysis to draw a more general conclusion, such as valence-arousal-dominance model [47].

## 6. Conclusion

In this study a new subject-independent EEG linear domain adaption method based on ELBN and DCNN is proposed. By scaling and translating EEG signal waves (i.e., linear mapping) to map the data in source domain to target domain, the EEG emotion recognition accuracy across individuals is considerably improved in both SEED and SEED-IV. The highest increment across frequency bands with ELBN and DCNN in SEED is up to 61.11% while the highest recognition accuracy can reach 97.22%. This improvement indicates that the wave forms between individual EEG data are highly similar so that the linear mapping can work effectively. Moreover, the scaling parameters and translation parameters are analyzed to figure out EEG emotion response mechanism. In statistical analysis results, channels interconnect to each other under the same frequency band, while those EEG data in different frequency bands are separated out. It is also found that the emotion complexity in experiments may influence the connection of channels. The more emotion categories are involved, the stronger correlation between channels can be led. Furthermore, those channels that are more likely to differ from others are prone to appearing at emotion insensitive brain cortex regions (i.e., parietal lobe and frontal lobe), which indicates that emotion sensitiveness of brain cortex region can influence the integration of intra-regional channels. Stronger emotion sensitiveness is related to stronger correlation between channels. In a word, this study provides an efficient approach to break the boundaries between subjects and reveals the EEG emotion response mechanism for future studies.

## References


[1] M. S. Özerdem, H. Polat, Emotion recognition based on eeg features in movie clips with channel selection, Brain informatics 4 (4) (2017) 241–252.

[2] S. Liu, Z. Wang, Y. An, J. Zhao, Y. Zhao, Y.-D. Zhang, Eeg emotion recognition based on the attention mechanism and pre-trained convolution capsule network, Knowledge-Based Systems 265 (2023) 110372.

[3] H. Cui, A. Liu, X. Zhang, X. Chen, K. Wang, X. Chen, Eeg-based emotion recognition using an end-to-end regional-asymmetric convolutional neural network, Knowledge-Based Systems 205 (2020) 106243.

[4] D. Dadebayev, W. W. Goh, E. X. Tan, Eeg-based emotion recognition: Review of commercial eeg devices and machine learning techniques, Journal of King Saud University-Computer and Information Sciences 34 (7) (2022) 4385–4401.

[5] E. H. Houssein, A. Hammad, A. A. Ali, Human emotion recognition from eeg-based brain–computer interface using machine learning: a comprehensive review, Neural Computing and Applications 34 (15) (2022) 12527–12557.

[6] M. R. Islam, M. A. Moni, M. M. Islam, M. Rashed-Al-Mahfuz, M. S. Islam, M. K. Hasan, M. S. Hossain, M. Ahmad, S. Uddin, A. Azad, et al., Emotion recognition from eeg signal focusing on deep learning and shallow learning techniques, IEEE Access 9 (2021) 94601–94624.

[7] J. Li, S. Qiu, Y.-Y. Shen, C.-L. Liu, H. He, Multisource transfer learning for cross-subject eeg emotion recognition, IEEE transactions on cybernetics 50 (7) (2019) 3281–3293.

[8] G. Li, D. Ouyang, Y. Yuan, W. Li, Z. Guo, X. Qu, P. Green, An eeg data processing approach for emotion recognition, IEEE Sensors Journal 22 (11) (2022) 10751–10763.

[9] J. Li, S. Qiu, C. Du, Y. Wang, H. He, Domain adaptation for eeg emotion recognition based on latent representation similarity, IEEE Transactions on Cognitive and Developmental Systems 12 (2) (2019) 344–353.

[10] D. Maheshwari, S. K. Ghosh, R. Tripathy, M. Sharma, U. R. Acharya, Automated accurate emotion recognition system using rhythm-specific deep convolutional neural network technique with multi-channel eeg signals, Computers in Biology and Medicine 134 (2021) 104428.

[11] T. Song, W. Zheng, P. Song, Z. Cui, Eeg emotion recognition using dynamical graph convolutional neural networks, IEEE Transactions on Affective Computing 11 (3) (2018) 532–541.

[12] Y. Yin, X. Zheng, B. Hu, Y. Zhang, X. Cui, Eeg emotion recognition using fusion model of graph convolutional neural networks and lstm, Applied Soft Computing 100 (2021) 106954.

[13] H. Cui, A. Liu, X. Zhang, X. Chen, K. Wang, X. Chen, Eeg-based emotion recognition using an end-to-end regional-asymmetric convolutional neural network, Knowledge-Based Systems 205 (2020) 106243.

[14] L. Yao, M. Wang, Y. Lu, H. Li, X. Zhang, Eeg-based emotion recognition by exploiting fused network entropy measures of complex networks across subjects, Entropy 23 (8) (2021) 984.

[15] C. Tan, M. Šarlija, N. Kasabov, Neurosense: Short-term emotion recognition and understanding based on spiking neural network modelling of spatio-temporal eeg patterns, Neurocomputing 434 (2021) 137–148.

[16] C. Yang, Z. Deng, K.-S. Choi, S. Wang, Takagi–sugeno–kang transfer learning fuzzy logic system for the adaptive recognition of epileptic electroencephalogram signals, IEEE Transactions on Fuzzy Systems 24 (5) (2015) 1079–1094.

[17] Z. Deng, P. Xu, L. Xie, K.-S. Choi, S. Wang, Transductive joint-knowledge-transfer tsk fs for recognition of epileptic eeg signals, IEEE Transactions on Neural Systems and Rehabilitation Engineering 26 (8) (2018) 1481–1494.

[18] J. Li, H. Hua, Z. Xu, L. Shu, X. Xu, F. Kuang, S. Wu, Cross-subject eeg emotion recognition combined with connectivity features and meta-transfer learning, Computers in biology and medicine 145 (2022) 105519.

[19] R. Zhou, Z. Zhang, H. Fu, L. Zhang, L. Li, G. Huang, Y. Dong, F. Li, X. Yang, Z. Liang, Pr-pl: A novel transfer learning framework with prototypical representation based pairwise learning for eeg-based emotion recognition, arXiv preprint arXiv:2202.06509 (2022).

[20] J. Quan, Y. Li, L. Wang, R. He, S. Yang, L. Guo, Eeg-based cross-subject emotion recognition using multi-source domain transfer learning, Biomedical Signal Processing and Control 84 (2023) 104741.

[21] R. Ning, C. P. Chen, T. Zhang, Cross-subject eeg emotion recognition using domain adaptive few-shot learning networks, in: 2021 IEEE International Conference on Bioinformatics and Biomedicine (BIBM), IEEE, 2021, pp. 1468–1472.

[22] W.-L. Zheng, B.-L. Lu, Investigating critical frequency bands and channels for eeg-based emotion recognition with deep neural networks, IEEE Transactions on autonomous mental development 7 (3) (2015) 162–175.

[23] P. Philippot, Inducing and assessing differentiated emotion-feeling states in the laboratory, Cognition and emotion 7 (2) (1993) 171–193.

[24] W.-L. Zheng, W. Liu, Y. Lu, B.-L. Lu, A. Cichocki, Emotionmeter: A multimodal framework for recognizing human emotions, IEEE transactions on cybernetics 49 (3) (2018) 1110–1122.

[25] D. Watson, L. A. Clark, A. Tellegen, Development and validation of brief measures of positive and negative affect: the panas scales., Journal of personality and social psychology 54 (6) (1988) 1063.

[26] D. Ouyang, Y. Yuan, G. Li, Z. Guo, The effect of time window length on eeg-based emotion recognition, Sensors 22 (13) (2022) 4939.

[27] H. Zhu, Z. Gu, H. Zhao, K. Chen, C.-T. Li, L. He, Developing a pattern discovery method in time series data and its gpu acceleration, Big Data Mining and Analytics 1 (4) (2018) 266–283.

[28] H. Sakoe, S. Chiba, Dynamic programming algorithm optimization for spoken word recognition, IEEE transactions on acoustics, speech, and signal processing 26 (1) (1978) 43–49.

[29] M. Cuturi, M. Blondel, Soft-dtw: a differentiable loss function for time-series, in: International conference on machine learning, PMLR, 2017, pp. 894–903.

[30] J. H. Zar, Spearman rank correlation: overview, Wiley StatsRef: Statistics Reference Online (2014).

[31] N. Nachar, et al., The mann-whitney u: A test for assessing whether two independent samples come from the same distribution, Tutorials in quantitative Methods for Psychology 4 (1) (2008) 13–20.

[32] H. Chen, M. Jin, Z. Li, C. Fan, J. Li, H. He, Ms-mda: Multisource marginal distribution adaptation for cross-subject and cross-session eeg emotion recognition, Frontiers in Neuroscience 15 (2021) 778488.

[33] J. Li, S. Li, J. Pan, F. Wang, Cross-subject eeg emotion recognition with self-organized graph neural network, Frontiers in Neuroscience 15 (2021) 611653.
[34] Z. Li, E. Zhu, M. Jin, C. Fan, H. He, T. Cai, J. Li, Dynamic domain adaptation for class-aware cross-subject and cross-session eeg emotion recognition, IEEE Journal of Biomedical and Health Informatics 26 (12) (2022) 5964–5973.
[35] Y. Peng, H. Liu, W. Kong, F. Nie, B.-L. Lu, A. Cichocki, Joint eeg feature transfer and semi-supervised cross-subject emotion recognition, IEEE Transactions on Industrial Informatics (2022).
[36] M. Jiménez-Guarneros, G. Fuentes-Pineda, Learning a robust unified domain adaptation framework for cross-subject eeg-based emotion recognition, Biomedical Signal Processing and Control 86 (2023) 105138.
[37] E. Lotfi, M.-R. Akbarzadeh-T, Practical emotional neural networks, Neural Networks 59 (2014) 61–72.
[38] J. C. Britton, K. L. Phan, S. F. Taylor, R. C. Welsh, K. C. Berridge, I. Liberzon, Neural correlates of social and nonsocial emotions: An fmri study, Neuroimage 31 (1) (2006) 397–409.
[39] A. Etkin, T. Egner, R. Kalisch, Emotional processing in anterior cingulate and medial prefrontal cortex, Trends in cognitive sciences 15 (2) (2011) 85–93.
[40] R. Oostenveld, P. Praamstra, The five percent electrode system for high-resolution eeg and erp measurements, Clinical neurophysiology 112 (4) (2001) 713–719.
[41] K. A. Lindquist, T. D. Wager, H. Kober, E. Bliss-Moreau, L. F. Barrett, The brain basis of emotion: a meta-analytic review, Behavioral and brain sciences 35 (3) (2012) 121–143.
[42] V. Padhmashree, A. Bhattacharyya, Human emotion recognition based on time–frequency analysis of multivariate eeg signal, Knowledge-Based Systems 238 (2022) 107867.
[43] J.-P. Lachaux, N. Axmacher, F. Mormann, E. Halgren, N. E. Crone, High-frequency neural activity and human cognition: past, present and possible future of intracranial eeg research, Progress in neurobiology 98 (3) (2012) 279–301.
[44] Z.-T. Liu, Q. Xie, M. Wu, W.-H. Cao, D.-Y. Li, S.-H. Li, Electroencephalogram emotion recognition based on empirical mode decomposition and optimal feature selection, IEEE Transactions on Cognitive and Developmental Systems 11 (4) (2018) 517–526.
[45] J. Wang, M. Wang, Review of the emotional feature extraction and classification using eeg signals, Cognitive robotics 1 (2021) 29–40.
[46] G. Cao, Y. Ma, X. Meng, Y. Gao, M. Meng, Emotion recognition based on cnn, in: 2019 Chinese Control Conference (CCC), IEEE, 2019, pp. 8627–8630.
[47] W. Li, R. Tan, Y. Xing, G. Li, S. Li, G. Zeng, P. Wang, B. Zhang, X. Su, D. Pi, et al., A multimodal psychological, physiological and behavioural dataset for human emotions in driving tasks, Scientific Data 9 (1) (2022) 481.
[48] G. Li, W. Yan, S. Li, X. Qu, W. Chu, D. Cao, A temporal–spatial deep learning approach for driver distraction detection based on eeg signals, IEEE Transactions on Automation Science and Engineering 19 (4) (2021) 2665–2677.